

Geophysical Research Letters

RESEARCH LETTER

10.1029/2021GL092518

Special Section:

The Arctic: An AGU Joint Special Collection

Key Points:

- March sea-level pressure (SLP) in 2020 was the lowest since 1948 over the Beaufort and Chukchi Seas
- Frequent and intense storms contributed to anomalous eastward sea ice motion in the region
- March 2020 continued a recent trend of Beaufort High collapse events as three of the four lowest March SLPs have occurred since 2017

Supporting Information:

Supporting Information may be found in the online version of this article.

Correspondence to:







T. J. Ballinger,
tjballinger@alaska.edu

Citation:

Ballinger, T. J., Walsh, J. E., Bhatt, U. S., Bieniek, P. A., Tschudi, M. A., Brettschneider, B., et al. (2021). Unusual west Arctic storm activity during winter 2020: Another collapse of the Beaufort High? *Geophysical Research Letters*, 48, e2021GL092518. <https://doi.org/10.1029/2021GL092518>

Received 20 JAN 2021
Accepted 29 MAY 2021

Unusual West Arctic Storm Activity During Winter 2020: Another Collapse of the Beaufort High?

Thomas J. Ballinger¹ , John E. Walsh¹, Uma S. Bhatt² , Peter A. Bieniek¹ , Mark A. Tschudi³, Brian Brettschneider⁴ , Hajo Eicken¹ , Andrew R. Mahoney² , Jackie Richter-Menge⁵, and Lewis H. Shapiro²

¹International Arctic Research Center, University of Alaska Fairbanks, Fairbanks, AK, USA, ²Geophysical Institute, University of Alaska Fairbanks, Fairbanks, AK, USA, ³Colorado Center for Astrodynamic Research, Department of Aerospace Engineering, University of Colorado Boulder, Boulder, CO, USA, ⁴NOAA/National Weather Service, Anchorage, AK, USA, ⁵Institute of Northern Engineering, University of Alaska Fairbanks, Fairbanks, AK, USA

Abstract Weather and sea ice forecasts provided in support of the U.S. Navy's Ice Exercise winter 2020 campaign in the Beaufort Sea noted frequent storms in the absence of the climatological Beaufort High which coincided with anomalous eastward drift of the region's ice cover. To place the 2020 Beaufort-Chukchi regional atmospheric conditions in historical context, we evaluated winter low sea-level pressure (SLP) extremes and storm characteristics in the region over the 1948–2020 period. March 2020 SLP in the Beaufort-Chukchi region was the lowest of the modern reanalysis era (1009.07 hPa) with record counts of passing storms and days with SLP at least two standard deviations below the climatological mean. The Beaufort High collapse in winter 2020 continued a recent pattern of Beaufort High collapses dating back to 2010. Unlike other recent collapses, such as 2017, most of the late-winter 2020 cyclones originated locally over the western Arctic Ocean.

Plain Language Summary Unusually stormy winter weather occurred in the southern Beaufort Sea during February and March 2020, affecting the U.S. Navy's Ice Exercise (ICEX) operations. Instead of the typical Beaufort High pressure pattern and associated easterly winds, frequent and at times intense storms moved across the Chukchi and Beaufort Seas, ushering westerly winds and eastward drift of sea ice and the ICEX camp. To quantify how unusual these weather conditions were, we evaluated storm activity from 1948 to 2020. March 2020 set a low pressure record for the month, in part because a record-number of intense storms that moved across the area. This storminess was supported by an unusually strong atmospheric circulation pattern over the Arctic Ocean that aided repetitive storm passage. Since 2010, the late-winter Beaufort High has been less common amidst more frequent storm activity, and three of the lowest four March mean sea-level pressure values on record have occurred during the last 4 years. This change in weather conditions has broad implications for the Arctic environment.

1. Introduction

The Beaufort Sea has a pivotal role in the decline of perennial Arctic sea ice and ocean-atmosphere interactions that both drive and respond to rapid sea-ice change (Babb et al., 2020; Mahoney et al., 2019; Petty et al., 2016; Proshutinsky et al., 2009). Specifically, the Beaufort Sea harbors some of the oldest and thickest multiyear ice advected out of the High Canadian Arctic as well as thinner ice produced in leads and polynyas within the southern Beaufort seasonal ice zone (Babb et al., 2020). The anticyclonic sea-level pressure (SLP) field and winds around the climatological Beaufort High drive the oceanic Beaufort Gyre circulation. The Beaufort High occurs throughout the year (Ballinger & Sheridan, 2014), though tends to be strongest during winter and spring (Serreze & Barrett, 2011). This feature is particularly crucial for controlling perennial ice transport across the broad Pacific Arctic sector. For example, westward ice drift and export are generally increasing in the southern Beaufort Sea as the ice pack becomes thinner and more mobile (Petty et al., 2016), but reversals occur due to the absence of the Beaufort High and Gyre which increase ice residence time in the region and hence ice accretion through growth and deformation (Babb et al., 2020). At the same time, advection of oceanic heat through Bering Strait and warm air masses from lower latitudes, residual summer ocean heat, and upwelling of Atlantic water are driven by atmospheric processes including storm activity (Danielson et al., 2020). These atmospheric processes are also tied to large-scale atmospheric

circulation and seasonal ice retreat patterns, which in turn impact the stability of the Beaufort High and Gyre (Armitage et al., 2020; Moore et al., 2018).

In this context, leading up to and during the U.S. Navy's Ice Exercise (ICEX) 2020 (McFarland, 2020), anomalous synoptic meteorological conditions in the Beaufort and Chukchi Seas were observed by an ICEX support team comprised of physical scientists from the University of Alaska Fairbanks in partnership with meteorologists and ice analysts from the U.S. National Ice Center and the Navy Fleet Weather Center. Weather and sea ice discussions frequently noted storm activity corresponding with anomalous westerly surface winds and resultant eastward ice drift across the Beaufort-Chukchi region, especially in the middle-to-end of March. Meteorological and environmental conditions during this period sharply contrasted those typically associated with the climatological Beaufort High and Gyre that tend to produce easterly surface winds and westward ice drift in the region during this time of year (Maeda et al., 2020; Petty et al., 2016; Serreze & Barrett, 2011).

The prolonged absence of the Beaufort High and Gyre during the ICEX 2020 campaign prompted the question as to how winter 2020 compared with previous years, including winter (hereon defined as the months of January, February, and March) of 2017 when the Beaufort High was said to have collapsed (Babb et al., 2020; Moore et al., 2018). The 2017 collapse was caused by the anomalous penetration of North Atlantic cyclones into the west Arctic which reversed the surface wind field and ice pack motion under record-high, westerly 10-m zonal winds of ~ 2 m/s and SLP values more than two standard deviations below normal (~ 1010 hPa) near the typical winter position of the Beaufort High (Moore et al., 2018).

Motivated by the seemingly unusual atmospheric dynamics behind the eastward Beaufort-Chukchi sea ice motion in winter 2020, we seek to place the Beaufort-Chukchi winter meteorological conditions in historical context. Our aim is to quantify the frequency, intensity, and duration of low SLPs in the region with respect to the 1948–2020 atmospheric reanalysis record. This analysis nearly doubles the temporal breadth of Moore et al.'s (2018) study covering 1979–2017 and seeks to explore whether individual Beaufort High collapse events, reported as episodic and anomalous, may be newly established, more persistent phenomena during winter (e.g., Babb et al., 2020) as such events and ice motion reversals until recently have been limited to summer (Asplin et al., 2009; Lukovich & Barber, 2006; Serreze et al., 1989). We concentrate our analysis on the late-winter period, including the period of ice camp operations during ICEX 2020.

With the above background as motivation, the goals of the present study are to:

1. Place the anomalous and unanticipated atmospheric conditions of late-winter 2020 into a longer historical perspective of variability and trends in the Beaufort-Chukchi region, and
2. Determine the large-scale atmospheric circulation features associated with the anomalous winds and ice drift in the Beaufort Sea during early 2020, thereby identifying the spatial scales of relevance to a diagnosis of short-term climatic extremes in the region.

Progress towards these two goals can provide some indication of the likelihood of an anomalous eastward wind regime and sea ice drift, thereby informing planners of future late-winter field operations in the Beaufort-Chukchi region and improving our understanding of the impact of recent atmospheric circulation anomalies on the Beaufort Sea ice pack.

2. Data and Methods

Weekly sea ice motion data from Tschudi, Meier, and Stewart (2019), Tschudi, Meier, Stewart, Fowler, and Maslanik (2019) and Tschudi et al. (2020) were used in the analysis. To create this product, multiple data sets were merged, including satellite retrievals from SMMR, SSM/I, SSMI/S, AVHRR, and AMSR-E, in situ IABP buoy data, and NCEP/NCAR Reanalysis forecasts. The resulting motion data were interpolated to a 25 km grid and averaged to produce this weekly sea ice motion product.

Daily mean SLP and geopotential height (GPH) data were obtained from NCEP/NCAR Reanalysis version 1 (NNR1; Kalnay et al., 1996) at the native 2.5° horizontal resolution from 1948 to 2020 ($n = 73$ years). Six-hourly NNR1 SLP data were additionally used for storm track analysis, which is detailed later in this section. To gain insight into the strength of the hemispheric-scale atmospheric circulation pattern, we also

examined the Arctic Oscillation (AO) index (Thompson & Wallace, 1998) from the NOAA Climate Prediction Center (CPC). The AO, also derived from NNR1 data, represents the leading empirical orthogonal function of 1000 hPa GPH anomalies (with respect to the 1979–2000 base period) over 20°N–90°N. NNR1 fields were used for consistency across our analyses and because SLP and GPH closely follow assimilated observational data streams (Kalnay et al., 1996).

SLP analyses were centered on the Beaufort-Chukchi study region defined as 70°N–85°N and 120°W–180°W, following Ballinger et al. (2014). Focus was placed on negative pressure anomalies and storms within this region by evaluating normalized daily SLP anomalies and applying a storm-tracking algorithm. The SLP anomalies were constructed in a simple, three-step process that involved: (a) averaging daily gridded SLP values within the study region, (b) subtracting out the 1981–2010 day-of-year (DOY) mean, and (c) dividing by the DOY standard deviation (σ) for the aforementioned climatological period. We subsequently documented the frequency of anomalous SLP days by calculating the monthly sum of $<0\sigma$ (i.e., less than the mean), $\leq -1\sigma$, and $\leq -2\sigma$ daily SLP anomalies within each month. We also performed duration analyses at the event scale by examining the persistence of daily SLP extremes of $\leq -1\sigma$, noting that more extreme criteria (i.e., days with $\text{SLP} \leq -2\sigma$) yielded fewer events. The occurrences of these events were documented over non-mutually exclusive 3–7 consecutive day windows (e.g., a 7d event was also counted as a 3, 4, ..., 6d event). The upper bound period was limited to 7d because events ≥ 8 d occur infrequently ($\leq 11\%$ of each winter month on average) over the reanalysis record.

We also utilized the storm tracking algorithm of Zhang et al. (2004) to document the number of closed low pressure systems entering the study region. This approach counts singular storm systems only once regardless of how often the same system enters or exits the specified domain. The storm tracks were derived from the 6-hourly NNR1 SLP data and subsequently aggregated to the monthly scale, with emphasis on the winter months akin to the time window of interest in the aforementioned study by Moore et al. (2018).

The Beaufort-Chukchi regional SLP time series were analyzed using simple descriptive statistics. Linear trends were calculated for running 30-year periods and statistical significance was determined from a two-tailed t-test when $p \leq 0.05$. A Poisson probability distribution was additionally used to evaluate the rarity of SLP anomaly occurrence for select time intervals.

3. Results

3.1. Sea Ice Drift, Surface Weather, and Atmospheric Circulation During Winter 2020

During March 2020 the Beaufort High was notably absent from its typical location in the western Arctic (Figure 1a). The anticyclone's absence in 2020 stood in sharp contrast to its climatological presence as an isolated high pressure cell of ~ 1020 hPa over the west Arctic Ocean (Figure 1b) with the most negative SLP anomalies propagating into the central and Siberian Arctic (Figure 1c). This collapse was influenced by a relatively elliptical polar jet stream over the Arctic basin (Figure 1d). The lack of a slight 500 hPa ridge over the West Arctic, which is a common upper-level feature supporting underlying March Beaufort High and Gyre development, further contributed to the unusual regional surface weather conditions (Figure 1e). As with SLP anomalies, the largest 500 hPa GPH anomalies were also pervasive across much of the Arctic Ocean, particularly north of 75°N and along the Siberian coastline (Figure 1f). This dipole anomaly pattern, indicative of the strong, large-scale pressure gradient, played a critical role in storm passage (described further in sections 3.2 and 3.3) and the absence of the climatological Beaufort High. In fact, the strong pressure gradient and zonal winds ascribed to this anomalous circulation pattern were captured by a record-high NOAA CPC winter AO index value of 2.83 (Ballinger et al., 2020). The pattern was remarkably persistent as indicated by the extreme, positive AO anomalies throughout the winter (CPC AO value [ascending rank since 1950] = 2.42 (3), 3.42 (1), and 2.64 (2) in January, February, and March, respectively).

Beaufort High collapse was further corroborated by anomalous westerly surface winds observed at Kak-tovik/Barter Island (Figure S1a) located along the southern Beaufort Sea coast just southwest of the ICEX camp's initial position (Figure S2). Relative to the climatological winds (Figure S1b), which exhibited a bimodal distribution of easterly and westerly component winds with few "extreme" occurrences ($\sim 5\%$ of wind observations exceeded 12 m/s), the March 2020 winds were relatively unimodal in direction (i.e., westerly) and "extreme" winds of ≥ 12 m/s occurred $\sim 30\%$ of the time.

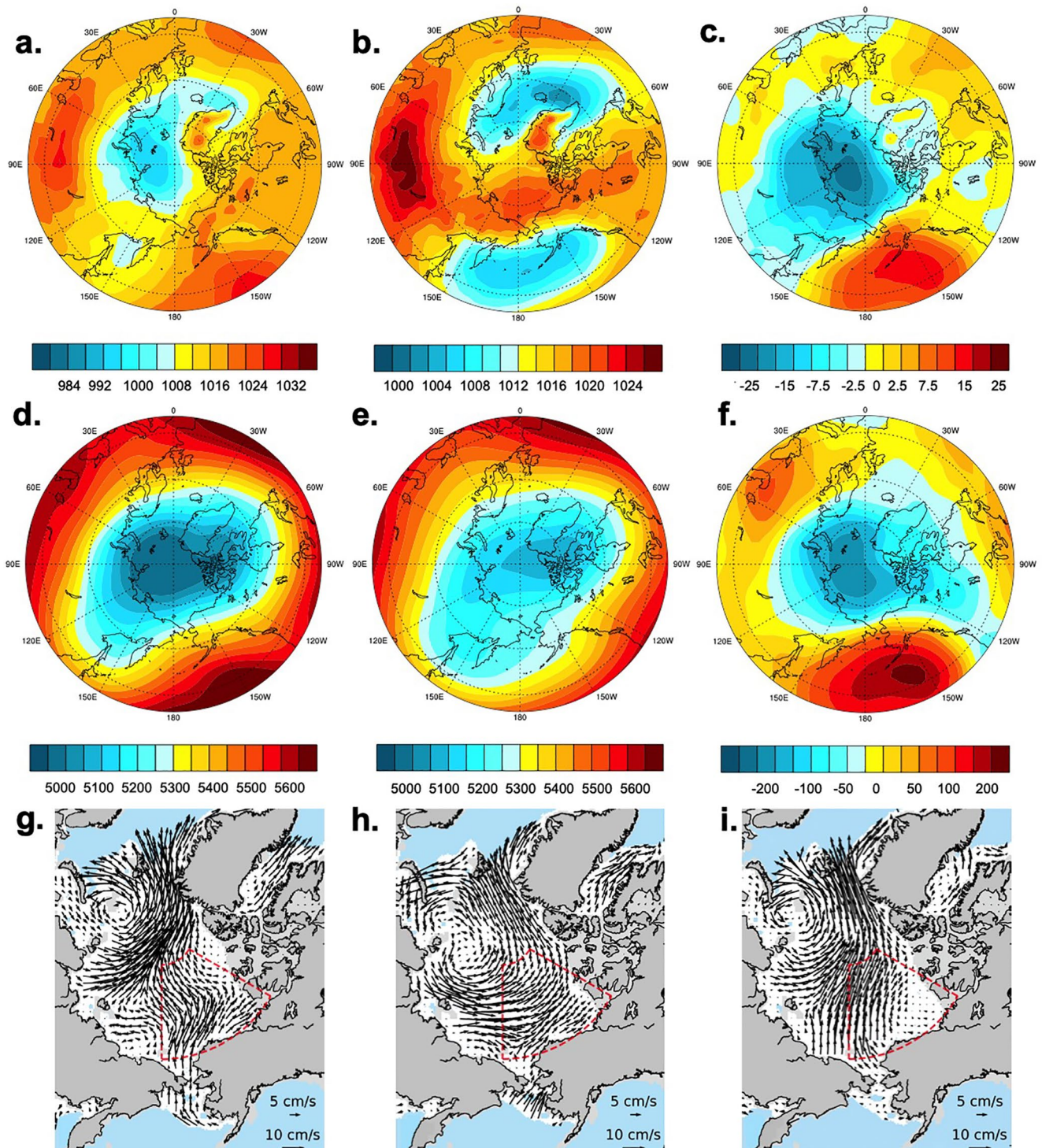


Figure 1. March sea-level pressure (SLP) fields (in hPa) for (a) 2020, (b) the 1981–2010 mean, and (c) 2020 anomaly (relative to the 1981–2010 mean). Similar maps, but for 500 hPa geopotential height fields (in m) are shown from left to right in (d–f). Weekly Arctic sea ice motion (in cm/s) for the last three weeks of March 2020 are also shown, which include (g) March 11–17, (h) March 18–24, and (i) March 25–31. White areas denote sea ice extent based on 15% sea ice concentration. The main study area (70°N–85°N, 120°W–180°W) is outlined by the red dashed polygon in (g–i) for which corresponding statistics are calculated for ice motion (Table S1) and SLP (Figures 2–4).

During the March 2020 collapse of the Beaufort High and large-scale atmospheric circulation anomalies, the Beaufort-Chukchi sea ice cover showed unusual drift (Figures 1g–1i; Table S1). Cyclonic activity and winds contributed to a reversal in the region's ice motion with enhanced eastward drift from March 11 to 24 (Figures 1g and 1h). This prolonged reversal largely drove the mean northeastward ice drift pattern observed for the month, specifically enhancing the eastward component (Figure S3). Further corroborating the anomalous Beaufort-Chukchi ice drift, an ice-tethered buoy at the ICEX camp in the southern Beaufort Sea measured total eastward drift of ~ 75 km during operations (Figure S2). From February 24 to March 28, 2020, the ICEX camp drifted eastward at an average speed of ~ 3 cm/s compared to the climatological mean drift speed of ~ 5 cm/s toward the west during March (Maeda et al., 2020).

3.2. Winter 2020 SLP in Historical Context

To place Beaufort-Chukchi winter 2020 conditions in a long-term perspective, we calculated the monthly mean SLP from daily data averaged over the 70°N – 85°N , 120°W – 180°W area. As shown by monthly SLP climatology marked by the gray dashed line in Figures 2a–2c, high pressure is common in the region and tends to increase through the progression of winter (e.g., January = 1016.75 hPa, February = 1018.60 hPa, and March = 1019.72 hPa). This can be attributed to this area's location within the polar cell and position under the northern extent of the North American ridge. With respect to monthly climatology, the mean SLP field over the Beaufort-Chukchi region in 2020 was below the 1981–2010 average in each winter month in 2020, with a gradual intensification of the negative pressure anomalies from January (-2.74 hPa) to February (-7.47 hPa) to March (-10.65 hPa). March 2020 SLP was the lowest value for the month on record (since 1948), and was 1.6 hPa lower than the previous record in 2017. Winter 2020 had the second lowest SLP (1011.40 hPa), narrowly behind 2017 (1011.23 hPa).

Record-low March SLP in 2020 was the result of a consistent occurrence of negative pressure anomalies throughout the month. March 2020 had the fourth fewest days of positive SLP anomalies ($n = 4\text{d}$; tied with 1990 and 1994 and trailed only 2019 [$n = 2\text{d}$] and 1986 [$n = 1\text{d}$], respectively, highlighted by a stretch of stormy weather late in the month that included daily SLP record minima on March 19 [997.74 hPa] and March 20 [992.20 hPa; Figure S4]). Three of the last four years (2017, 2019, and 2020) represented three of the four lowest March mean SLP values of the reanalysis era. This series of anomalous years continued a pattern of prevailing late-winter negative SLP anomalies since 2010 where 7 and 8 of the last 11 February and March months, respectively, exhibited negative SLP anomalies. Using a Poisson distribution, the probability of such SLP frequencies within any 11-year period between 1948–2020 was 15% in February, but only 7% for March. This highlights the rarity with which negative SLP anomalies have characterized recent winters. Such anomalies have also prompted an inflection in the 30-year February and March SLP trends (Figures 2e and 2f). For March specifically, this abrupt change in the trend sign and magnitude followed a period of consistent, positive SLP anomalies across the late-1990s and late-2000s that raised 30-year trends to peak and statistically significant levels before the onset of recent storm activity (Figure 2f).

3.3. Frequency and Persistence of Storm Activity

Winter 2020 pressure anomalies were further placed in context by examining the incidence of extreme days and events at different normalized SLP thresholds. Daily occurrences of regional SLP $< 0\sigma$, $\leq -1\sigma$, and $\leq -2\sigma$ for each winter month are documented in Figures 3a–3c. February 2020 tied with 2011 for the highest count of days with SLP $< 0\sigma$ ($n = 25\text{d}$; Figure 3b). The incidence of anomalous SLP days in February continued into March with the fourth highest count (tied with 1994) of days with SLP $< 0\sigma$ ($n = 27\text{d}$) and the second-highest count of SLP $\leq -1\sigma$ days ($n = 16\text{d}$). Further, March of 2020 saw particularly strong storms in the region and tied March of both 1993 and 2007 for record-high occurrence ($n = 5\text{d}$) of extreme SLP anomalies ($\leq -2\sigma$; Figure 3c). For reference, the daily mean SLP of these March 2020 extreme storms ranged between 992.20–1002.60 hPa for the aforementioned stormy period on March 19–20 and 23–25 (Figure S4).

Given high incidence and clustering of low SLP extremes, was the persistence of these conditions anomalous in winter 2020? The occurrence of SLP extremes $\leq -1\sigma$ lasting 3–7 consecutive days is captured in Figures 3d–3f. Despite record or near-record negative SLP anomalies for February and March 2020, event frequencies within these months did not set records. In February, there was above-average occurrence of

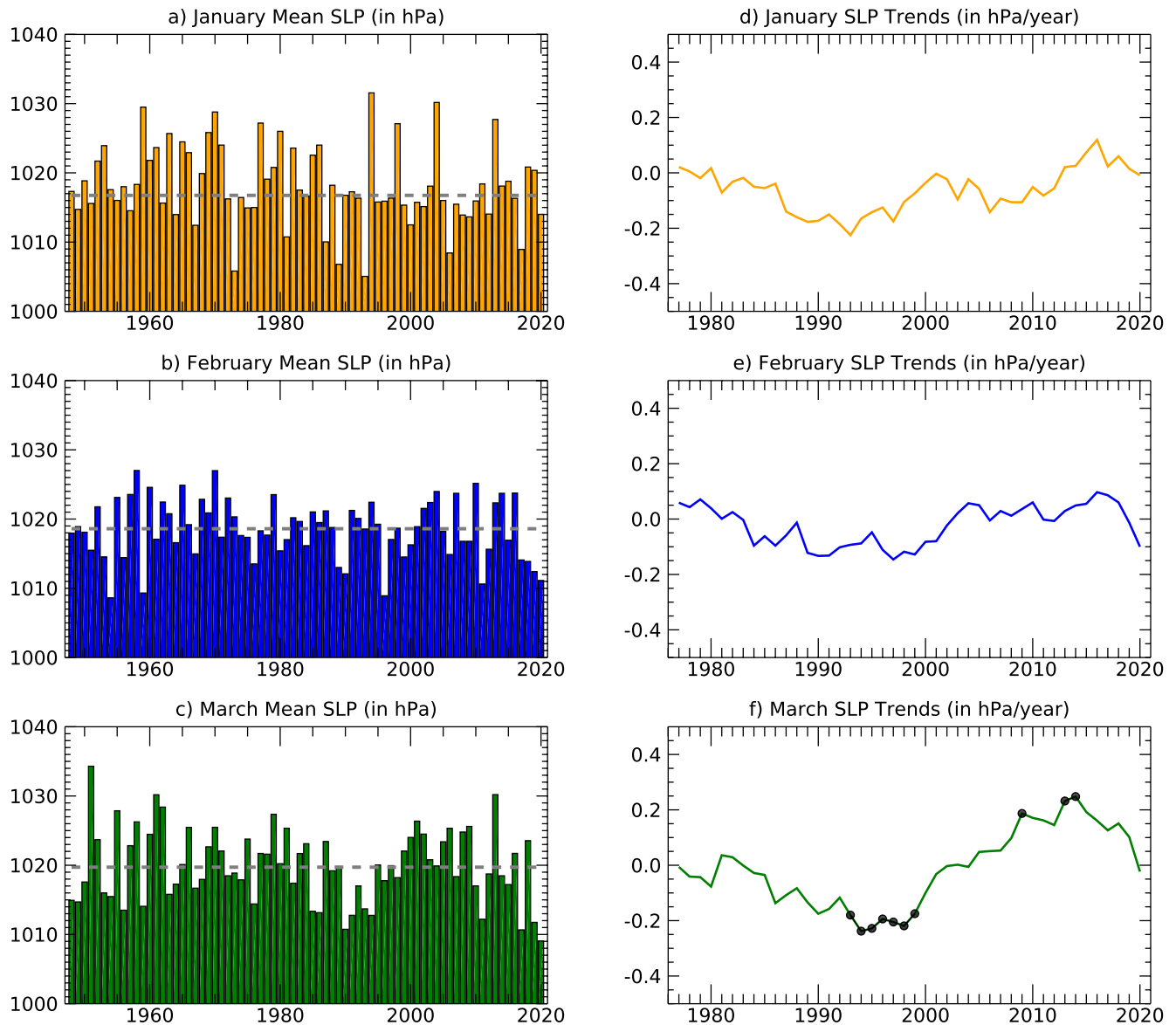


Figure 2. Regional mean sea-level pressure (SLP) (a–c), 1948–2020, and (d–f) running 30-year trends in the mean SLP for each winter month. In (a–c), the 1981–2010 monthly mean SLP is indicated by the gray dashed reference line. Each trend value in (d–f) represents the final year of the running period (e.g., 1977 = trend for the 1948–1977 period inclusive). Significant trend periods ($p \leq 0.05$ for $n-2$ degrees of freedom) are marked by black dots.

events lasting 3d ($n = 4$), 4d ($n = 3$), and 5d ($n = 3$), but these counts all trail years of greater persistence in the 1950s and 1970s (Figure 3e). Similarly for March, 3d ($n = 8$), 4d ($n = 6$), and 5d ($n = 4$) events all rank at or above the 90th percentile for event frequency, but were exceeded by several years since the mid-1980s (Figure 3f).

Applying the Zhang et al. (2004) algorithm, storm track analysis further indicated that March 2020 storminess in the Beaufort-Chukchi region was remarkable (Figure 4a), tying 1954 and 1998 ($n = 11$ storms) with record-high normalized cyclone counts of two standard deviations above the 1981–2010 mean. Most of these storms formed locally, that is within or immediately west of the Beaufort-Chukchi region (Figure 4b). On the Arctic scale (north of 65°N), the frequency of March storms relative to the historical record was also elevated, but not record-setting as was found within the Beaufort-Chukchi area. Unlike 2020, the 2017 Beaufort High collapse analog saw fewer March storms and those that formed mainly originated in the North Atlantic and North American Arctic before migrating into the Beaufort-Chukchi region (Figure 4b). When

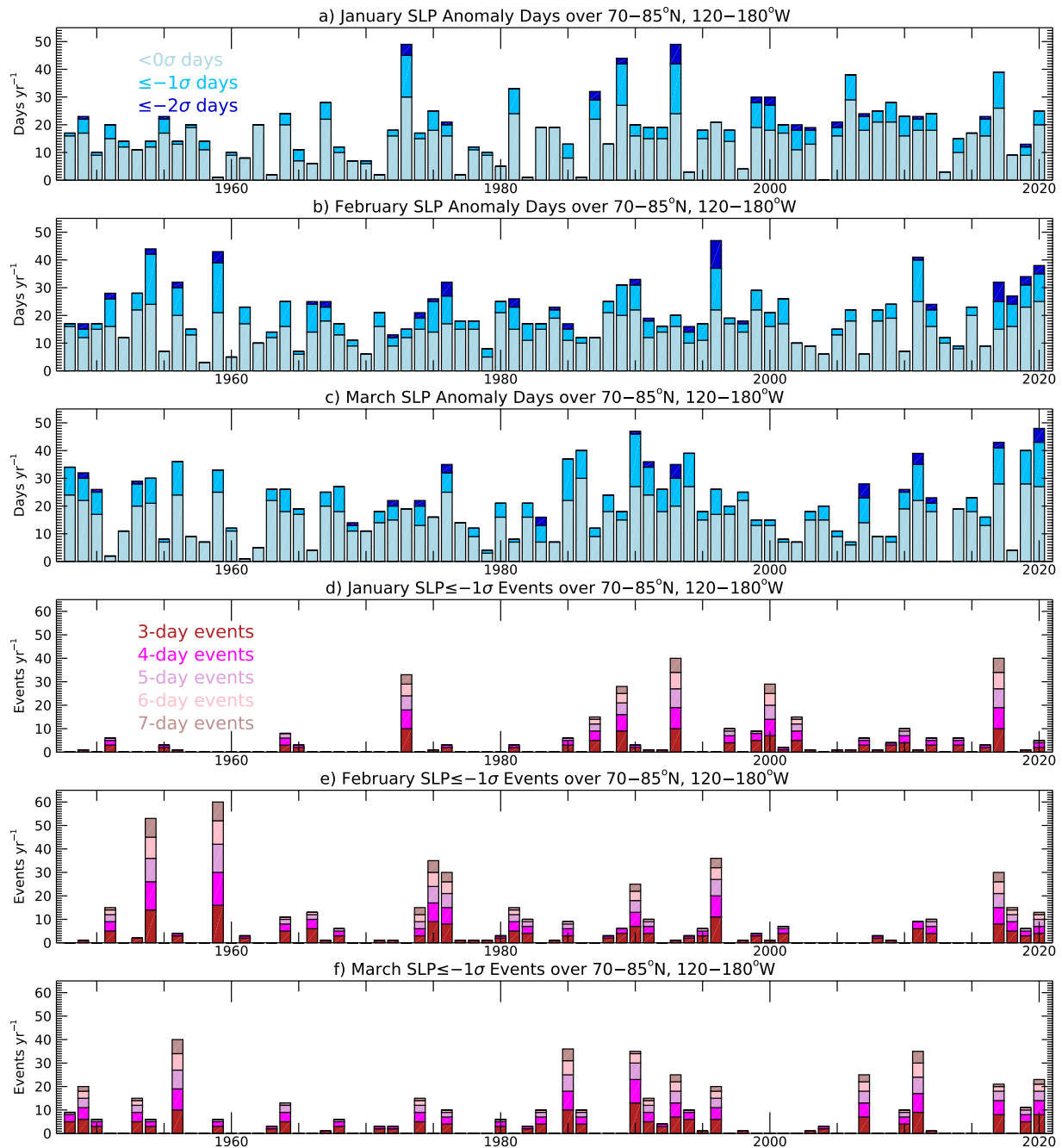


Figure 3. Counts of January–March sea-level pressure (SLP) anomaly days based on different (a–c) normalized SLP thresholds and (d–f) SLP $\leq -1\sigma$ events, which last for $n = 3, 4, \dots, 7$ days. Stacked bars represent discretized counts and are cumulative across the categories for each year (e.g., March 2020 had 27 days of domain-averaged SLP $< 0\sigma$ of which 16 of those days were $\leq -1\sigma$ and five of the days were $\leq -2\sigma$).

comparing cyclone activity across the winter season of these two collapse years, some clear similarities and differences emerge. The 2017 collapse was characterized by more frequent early season (January–February) storms relative to 2020 (Figure 4c). However, there were not demonstrable differences between the number of storms forming upstream over the North Atlantic and Siberian coasts in these years (Figure 4d). Our analyses suggest that cyclogenesis geography in winter 2017 was similar to that of 2020 with one difference being a cluster of winter 2017 storms that formed in and around the Bering Sea (Figure 4d).

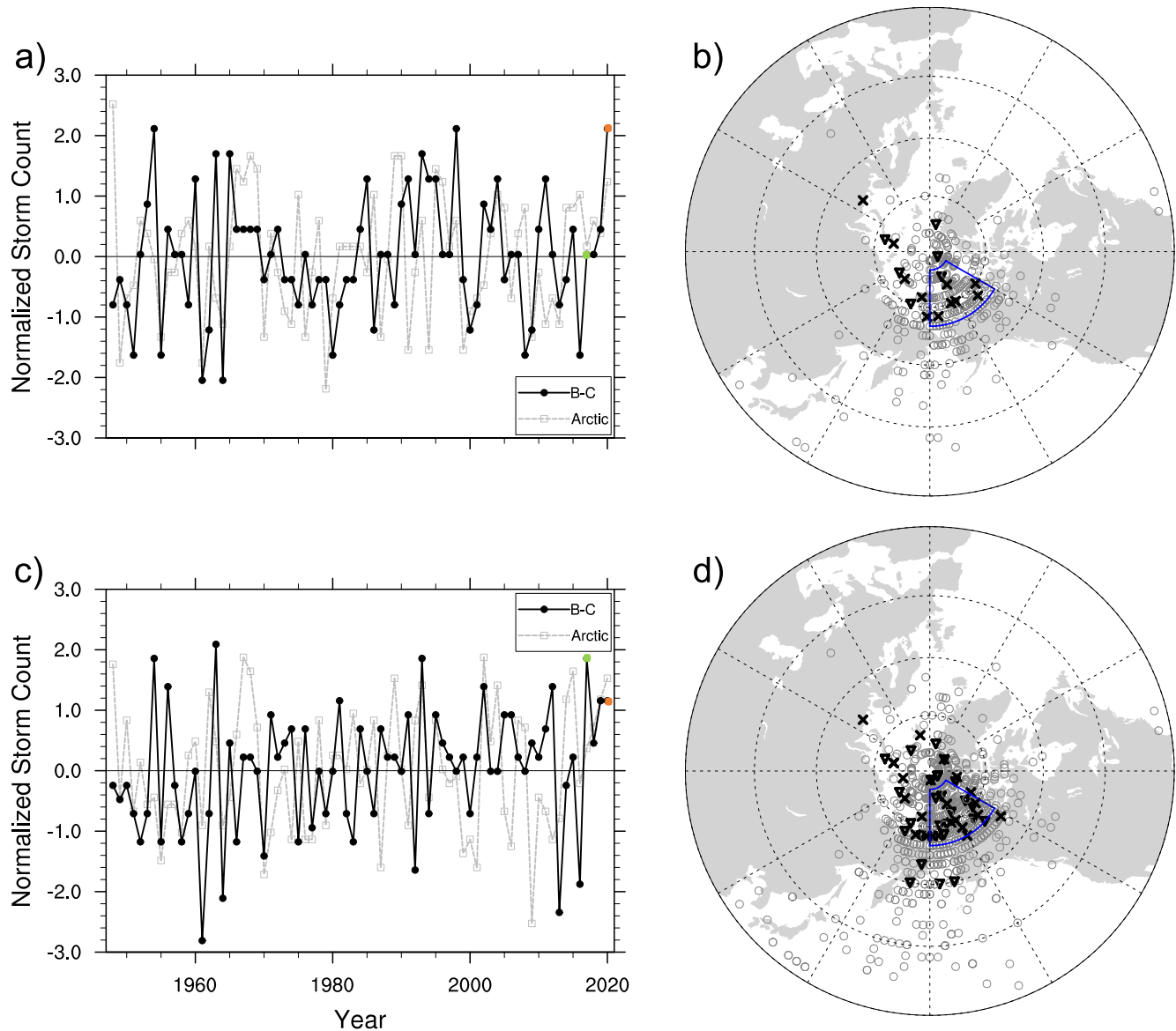


Figure 4. Time series of March normalized storm counts are shown in (a) from 1948–2020 with respect to the 1981–2010 climatology for the Beaufort-Chukchi region and the Arctic (areas north of 65°N). In (b), the cyclogenesis location of each storm that subsequently moved into the Beaufort-Chukchi region (blue polygon) is identified for March 2017 (each black triangle) and March 2020 (each black “x”). March storms from other years dating back to 1948 are shown by gray circles. Similar time series and cyclogenesis plots are shown for winter (January–March) in (c) and (d), respectively with 2017 (2020) marked by a green (orange) dot.

4. Discussion and Conclusions

Through analyses of multiple metrics and atmospheric fields, we found that anomalous eastward ice motion observed in the Beaufort-Chukchi region during March 2020 was the result of increased storminess and associated collapse of the Beaufort High. Through addressing the first goal of our study, we found that the regional SLP (70°N–85°N, 120°W–180°W) was the lowest monthly mean (1009.07 hPa), nearly 2 hPa lower than the previous record in 2017, and was marked by a near-record for $SLP \leq -1\sigma$ days and a record-tying number of $SLP \leq -2\sigma$ days and storms tracking into the region. Forecast discussions held in support of ICEX 2020 regularly noted the atypical, seasonal frequency of cyclonic systems in the absence of the climatological Beaufort High. Westerly winds on the southern flanks of these storms drove eastward camp drift counter to westward climatological ice motion of the southern Beaufort Sea (Maeda et al., 2020). Our analyses showed that the frequency of late-winter low pressure extremes, but not their duration, was

unusual with respect to the reanalysis record. Three of the last four years (2017, 2019, and 2020) highlight a recent pattern of uncommonly low March regional SLP. Furthermore, areal SLP was lower and storms were more frequent in 2020 than during the previous March low SLP record of 2017. Storm track analyses also suggested that cyclone activity during the 2020 reversal of the Beaufort Gyre and collapse of the Beaufort High was more pronounced in March compared to the 2017 collapse, while the latter case exhibited more frequent winter storms within January and February.

With regards to our second study goal, we found that in addition to the collapsed Beaufort High and enhanced storminess in late-winter 2020, other synoptic meteorological features were instrumental in supporting storm passage and eastward ice drift, namely the large-scale dipole anomaly between low pressure centered on the Siberian Arctic coastline and high pressure located over high-latitude lands, especially Alaska. This pattern supported westerly, geostrophic winds that allowed for frequent and rapid transit of cyclonic systems through the region. March cyclogenesis was also local to the Pacific Arctic sector in 2020 likely due to the baroclinic environment supported by the quasi-stationary SLP dipole between the Siberian coast and continental Alaska. Yet another striking feature of winter 2020 was the West Arctic's response to a persistent, strongly positive AO regime and contracted polar jet stream and vortex. Studies have long noted that despite positive winter AO extremes (i.e., $AO \geq 1$), with widespread low pressure across the Arctic Basin, a weakened Beaufort High and Gyre tended to occur to produce slow, easterly, alongshore winds north of Alaska (Kwok et al., 2013; Rigor et al., 2002). In late-winter 2020, the Beaufort-Chukchi region did not demonstrate such a response to the hemispheric circulation anomaly. In particular, the Beaufort High was absent in March (Figure 4e), a month in which it is climatologically a prominent feature (Figure 4a).

Unusual winter 2020 weather conditions warrant follow-up analysis regarding the extent to which the Beaufort High's collapse and record storm activity subsequently impacted the region's interconnected physical system, particularly in light of documented lags between atmospheric anomalies and the response of sea ice, energy, and freshwater budgets (Armitage et al., 2020; Babb et al., 2019; Polyakov et al., 2020). While such sea ice reversals under an absent Beaufort High historically have tended to promote dynamic ice pack thickening and impede summer ice loss, a recent case study of winter 2017 by Babb et al. (2020) showed that spring dynamic forcing overrode this winter ocean-atmosphere preconditioning. Analysis of winter 2020 and future reversal events as it relates to sea ice preconditioning for subsequent melt seasons is necessary to better understand the evolution of West Arctic ice-ocean coupling in a changing climate. Finally, analysis of model projections of future changes of Beaufort High collapses would be timely. For meaningful conclusions about future changes, however, one would need to demonstrate that the models' historical simulations capture the Beaufort High's seasonal and interannual variability.

Data Availability Statement

NNR1 reanalysis data are publicly available from NOAA PSL at <https://psl.noaa.gov/data/gridded/data.ncep.reanalysis.html>. Referenced NOAA CPC AO index values can be found at https://www.cpc.ncep.noaa.gov/products/precip/CWlink/daily_ao_index/ao.shtml. The sea ice motion data through 2019 are available from NSIDC at <https://nsidc.org/data/NSIDC-0116/versions/4>. The 2020 sea ice motion data are available as Quick Look files, found at <https://nsidc.org/data/NSIDC-0748/versions/1>. Kaktovik/Barter Island AWOS data and plotting tools are available at <https://mesonet.agron.iastate.edu/>. New data analyzed in this manuscript and not otherwise publicly archived, which includes the ICEX camp drift coordinates (Figure 1) and storm counts (Figure 4), can be found at Mendeley Data (<https://data.mendeley.com/datasets/8n72vcn3x4/1>).

Acknowledgments

The authors acknowledge support from the U.S. Navy Arctic Submarine Laboratory. T. J. Ballinger is additionally supported by the UAF Experimental Arctic Prediction Initiative. We thank J. Scott Stewart (NSIDC) for assistance with Figure 1. We appreciate the time and suggestions of two anonymous reviewers and the editor, Gudrun Magnúsdóttir, which have aided the improvement of our manuscript.

References

- Armitage, T. W. K., Manucharyan, G. E., Petty, A. A., Kwok, R., & Thompson, A. F. (2020). Enhanced eddy activity in the Beaufort Gyre in response to sea ice loss. *Nature Communications*, 11, 1–8. <https://doi.org/10.1038/s41467-020-14449-z>
- Asplin, M. G., Lukovich, J. V., & Barber, D. G. (2009). Atmospheric forcing of the Beaufort Sea ice gyre: Surface pressure climatology and sea ice motion. *Journal of Geophysical Research*, 114, C00A06. <https://doi.org/10.1029/2008JC005127>
- Babb, D. G., Landy, J. C., Barber, D. G., & Galley, R. J. (2019). Winter sea ice export from the Beaufort Sea as a preconditioning mechanism for enhanced summer melt: A case study of 2016. *Journal of Geophysical Research: Oceans*, 124, 6575–6600. <https://doi.org/10.1029/2019jc015053>

- Babb, D. G., Landy, J. C., Lukovich, J. V., Haas, C., Hendricks, S., Barber, D. G., & Galley, R. J. (2020). The 2017 reversal of the Beaufort Gyre: Can dynamic thickening of a seasonal ice cover during a reversal limit summer ice melt in the Beaufort Sea? *Journal of Geophysical Research: Oceans*, *125*, e2020JC016796. <https://doi.org/10.1029/2020JC016796>
- Ballinger, T. J., Overland, J. E., Wang, M., Bhatt, U. S., Hanna, E., Hanssen-Bauer, I., et al. (2020). Surface air temperature. In R. L. Thoman, J. Richter-Menge, & M. L. Druckenmiller (Eds.), NOAA Arctic report card 2020. <https://doi.org/10.25923/gcw8-2z06>
- Ballinger, T. J., & Sheridan, S. C. (2014). Associations between circulation pattern frequencies and sea ice minima in the western Arctic. *International Journal of Climatology*, *34*, 1385–1394. <https://doi.org/10.1002/joc.3767>
- Ballinger, T. J., Sheridan, S. C., & Hanna, E. (2014). Resolving the Beaufort Sea High using synoptic climatological methods. *International Journal of Climatology*, *34*, 3312–3319. <https://doi.org/10.1002/joc.3907>
- Danielson, S. L., Ahkinga, O., Ashjian, C., Basyuk, E., Cooper, L. W., Eisner, L., et al. (2020). Manifestation and consequences of warming and altered heat fluxes over the Bering and Chukchi Sea continental shelves. *Deep-Sea Research Part II*, *177*, 1–22. <https://doi.org/10.1016/j.dsr2.2020.104781>
- Kalnay, E., Kanamitsu, M., Kistler, R., Collins, W., Deaven, D., Gandin, L., et al. (1996). The NCEP/NCAR 40-year reanalysis project. *Bulletin of the American Meteorological Society*, *77*, 437–471. [https://doi.org/10.1175/1520-0477\(1996\)077<0437:tnyrp>2.0.co;2](https://doi.org/10.1175/1520-0477(1996)077<0437:tnyrp>2.0.co;2)
- Kwok, R., Spreen, G., & Pang, S. (2013). Arctic sea ice circulation and drift speed: Decadal trends and ocean currents. *Journal of Geophysical Research: Oceans*, *118*, 2408–2425. <https://doi.org/10.1002/jgrc.20191>
- Lukovich, J. V., & Barber, D. G. (2006). Atmospheric controls on sea ice motion in the southern Beaufort Sea. *Journal of Geophysical Research*, *111*, D18103. <https://doi.org/10.1029/2005JD006408>
- Maeda, K., Kimura, N., & Yamaguchi, H. (2020). Temporal and spatial changes in the relationship between sea-ice motion and wind in the Arctic. *Polar Research*, *39*, 1–10. <https://doi.org/10.33265/polar.v39.3370>
- Mahoney, A. R., Hutchings, J. K., Eicken, H., & Haas, C. (2019). Changes in the thickness and circulation of multiyear ice in the Beaufort Gyre determined from pseudo-Lagrangian methods from 2003–2015. *Journal of Geophysical Research: Oceans*, *124*, 5618–5633. <https://doi.org/10.1029/2018jc014911>
- McFarland, H. (2020). UAF scientists lend expertise to Navy's Arctic ice camp. 6 March 2020. Retrieved from <https://uaf-iarc.org/2020/03/06/uaf-scientists-lend-expertise-to-navys-arctic-ice-camp/>
- Moore, G. W. K., Schweiger, A., Zhang, J., & Steele, M. (2018). Collapse of the 2017 winter Beaufort High: A response to thinning sea ice? *Geophysical Research Letters*, *45*, 2860–2869. <https://doi.org/10.1002/2017gl076446>
- Petty, A. A., Hutchings, J. K., Richter-Menge, J. A., & Tschudi, M. A. (2016). Sea ice circulation around the Beaufort Gyre: The changing role of wind forcing and the sea ice state. *Journal of Geophysical Research: Oceans*, *121*, 3278–3296. <https://doi.org/10.1002/2015jc010903>
- Polyakov, I. V., Alkire, A. B., Bluhm, B. A., Brown, K. A., Carmack, E. C., Chierici, M., et al. (2020). Borealization of the Arctic Ocean in response to anomalous advection from sub-Arctic Seas. *Frontiers in Marine Science*, *7*, 1–32. <https://doi.org/10.3389/fmars.2020.00491>
- Proshutinsky, A., Krishfield, R., Timmermans, M.-L., Toole, J., Carmack, E., McLaughlin, F., et al. (2009). Beaufort Gyre freshwater reservoir: State and variability from observations. *Journal of Geophysical Research*, *114*, 1–25. <https://doi.org/10.1029/2008jc005104>
- Rigor, I. G., Wallace, J. M., & Colony, R. L. (2002). Response of sea ice to the Arctic Oscillation. *Journal of Climate*, *15*, 2648–2663. [https://doi.org/10.1175/1520-0442\(2002\)015<2648:rositt>2.0.co;2](https://doi.org/10.1175/1520-0442(2002)015<2648:rositt>2.0.co;2)
- Serreze, M. C., & Barrett, A. P. (2011). Characteristics of the Beaufort Sea High. *Journal of Climate*, *24*, 159–182. <https://doi.org/10.1175/2010jcli3636.1>
- Serreze, M. C., Barry, R. G., & McLaren, A. S. (1989). Seasonal variations in sea ice motion and effects on sea ice concentration in the Canada Basin. *Journal of Geophysical Research*, *94*, 10955–10970. <https://doi.org/10.1029/jc094ic08p10955>
- Thompson, D. W. J., & Wallace, J. M. (1998). The Arctic Oscillation signature in the wintertime geopotential height and temperature fields. *Geophysical Research Letters*, *25*, 1297–1300. <https://doi.org/10.1029/98gl00950>
- Tschudi, M., Meier, W. N., & Stewart, J. S. (2019). *Quicklook Arctic weekly EASE-Grid Sea ice motion vectors, version 1*. Boulder, Colorado USA: NASA National Snow and Ice Data Center Distributed Active Archive Center. <https://doi.org/10.5067/O0X18PPYEZJ6>
- Tschudi, M., Meier, W. N., Stewart, J. S., Fowler, C., & Maslanik, J. (2019). *Polar Pathfinder daily 25 km EASE-Grid Sea ice motion vectors, version 4*. Boulder, Colorado USA: NASA National Snow and Ice Data Center Distributed Active Archive Center. <https://doi.org/10.5067/INAWUWO7QH7B>
- Tschudi, M. A., Meier, W. N., & Stewart, J. S. (2020). An enhancement to sea ice motion and age products at the National Snow and Ice Data Center (NSIDC). *The Cryosphere*, *14*, 1519–1536. <https://doi.org/10.5194/tc-14-1519-2020>
- Zhang, X. D., Walsh, J. E., Zhang, J., Bhatt, U. S., & Ikeda, M. (2004). Climatology and interannual variability of arctic cyclone activity: 1948–2002. *Journal of Climate*, *17*, 2300–2317. [https://doi.org/10.1175/1520-0442\(2004\)017<2300:caivoa>2.0.co;2](https://doi.org/10.1175/1520-0442(2004)017<2300:caivoa>2.0.co;2)

References From the Supporting Information

- Barber, D. G., McCullough, G., Babb, D., Komarov, A. S., Candlish, L. M., Lukovich, J. V., et al. (2014). Climate change and ice hazards in the Beaufort Sea. *Elementa: Science of the Anthropocene*, *2*, 1–13. <https://doi.org/10.12952/journal.elementa.000025>
- Dammann, D. O., Eicken, H., Mahoney, A. R., Meyer, F. J., & Betcher, S. (2018). Assessing sea ice trafficability in a changing Arctic. *Arctic*, *71*, 59–75. <https://doi.org/10.14430/arctic4701>
- Dezutter, T., Lalande, C., Dufresne, C., Darnis, G., & Fortier, L. (2019). Mismatch between microalgae and herbivorous copepods due to the record sea ice minimum extent of 2012 and the late sea ice break-up of 2013 in the Beaufort Sea. *Progress in Oceanography*, *173*, 66–77. <https://doi.org/10.1016/j.pocean.2019.02.008>
- Eicken, H., & Mahoney, A. R. (2015). Sea ice: Hazards, risks, and implications for disasters. *Coastal and Marine Hazards, Risks, and Disasters*, 381–401. Elsevier. <https://doi.org/10.1016/b978-0-12-396483-0.00013-3>
- Ziezulewicz, G. (2020). In a thawing era, ICEX 2020 kicks off up north (5 March 2020). Navy Times. Retrieved from <https://www.navytimes.com/news/your-navy/2020/03/05/in-a-thawing-era-icex-2020-kicks-off-up-north/>